https://ntrs.nasa.gov/search.jsp?R=20140004054 2019-08-29T14:22:44+00:00Z

NASA/TM-2014-218243

Modeling and Simulation of Upset-Inducing Disturbances for Digital Systems in an Electromagnetic Reverberation Chamber

Wilfredo Torres-Pomales
Langley Research Center, Hampton, Virginia

April 2014

NASA STI Program . . . in Profile

Since its founding, NASA has been dedicated to the advancement of aeronautics and space science. The NASA scientific and technical information (STI) program plays a key part in helping NASA maintain this important role.

The NASA STI program operates under the auspices of the Agency Chief Information Officer. It collects, organizes, provides for archiving, and disseminates NASA's STI. The NASA STI program provides access to the NASA Aeronautics and Space Database and its public interface, the NASA Technical Report Server, thus providing one of the largest collections of aeronautical and space science STI in the world. Results are published in both non-NASA channels and by NASA in the NASA STI Report Series, which includes the following report types:

- TECHNICAL PUBLICATION. Reports of completed research or a major significant phase of research that present the results of NASA Programs and include extensive data or theoretical analysis. Includes compilations of significant scientific and technical data and information deemed to be of continuing reference value. NASA counterpart of peer-reviewed formal professional papers, but having less stringent limitations on manuscript length and extent of graphic presentations.

- TECHNICAL MEMORANDUM. Scientific and technical findings that are preliminary or of specialized interest, e.g., quick release reports, working papers, and bibliographies that contain minimal annotation. Does not contain extensive analysis.

- CONTRACTOR REPORT. Scientific and technical findings by NASA-sponsored contractors and grantees.

- CONFERENCE PUBLICATION. Collected papers from scientific and technical conferences, symposia, seminars, or other meetings sponsored or co-sponsored by NASA.

- SPECIAL PUBLICATION. Scientific, technical, or historical information from NASA programs, projects, and missions, often concerned with subjects having substantial public interest.

- TECHNICAL TRANSLATION. English-language translations of foreign scientific and technical material pertinent to NASA's mission.

Specialized services also include organizing and publishing research results, distributing specialized research announcements and feeds, providing information desk and personal search support, and enabling data exchange services.

For more information about the NASA STI program, see the following:

- Access the NASA STI program home page at *http://www.sti.nasa.gov*

- E-mail your question to help@sti.nasa.gov

- Fax your question to the NASA STI Information Desk at 443-757-5803

- Phone the NASA STI Information Desk at 443-757-5802

- Write to:
  STI Information Desk
  NASA Center for AeroSpace Information
  7115 Standard Drive
  Hanover, MD 21076-1320

NASA/TM-2014-218243

Modeling and Simulation of Upset-Inducing Disturbances for Digital Systems in an Electromagnetic Reverberation Chamber

Wilfredo Torres-Pomales
Langley Research Center, Hampton, Virginia

National Aeronautics and
Space Administration

Langley Research Center
Hampton, Virginia 23681-2199

April 2014

Acknowledgment

The author is grateful for the comments and suggestions by Dr. Van E. Brewer of Old Dominion University, and Kenneth W. Eure, Truoung X. Nguyen, Laura J. Smith and Allan L. White of NASA Langley Research Center.

Available from:

NASA Center for AeroSpace Information
7115 Standard Drive
Hanover, MD 21076-1320
443-757-5802

Abstract

This report describes a modeling and simulation approach for disturbance patterns representative of the environment experienced by a digital system in an electromagnetic reverberation chamber. The disturbance is modeled by a multivariate statistical distribution based on empirical observations. Extended versions of the Rejection Samping and Inverse Transform Sampling techniques are developed to generate multivariate random samples of the disturbance. The results show that Inverse Transform Sampling returns samples with higher fidelity relative to the empirical distribution. This work is part of an ongoing effort to develop a resilience assessment methodology for complex safety-critical distributed systems.

Table of Contents

1. Introduction

A research effort is underway to develop practical validation and verification (V&V) methods that can enable rigorous safety assurance for the next generation of aviation systems. These systems are characterized by highly complex, large-scale, network-based distributed architectures with software-implemented functionality and advanced computation and communication capabilities. To meet the safety goals, these systems must be demonstrably robust with respect to system design and implementation errors, component degradations and failures, and partial system failures. The V&V challenge is compounded by strong coupling of system components in the software and the hardware, as well as the need to consider unexpected and possibly malicious component behavior [1].

To support this research effort, verification approaches are being developed for robust distributed algorithms that support system resource management in a fault space with a wide range of severity. A system architecture for safety-critical real-time applications must have the ability to mitigate the effects of internal component faults of varying severity [2]. A safety-critical system must have sufficient tolerance to accommodate more frequent uncorrelated random faults without disruption of the system services. A robust system must also mitigate infrequent but more severe correlated faults that can exceed the system design assumptions, disrupt internal coordinated operation among the system components and propagate effects outward to the external service interfaces. Analysis techniques will be developed for system designs intended to ensure continued safe operation in the presence of component misbehavior while simultaneously minimizing their adverse effects. These techniques should enable designs with strongly assured safety properties under the weakest possible (i.e., least restrictive) assumptions in terms of the number and types of faults a system can handle.

In this context, we are developing analysis and simulation tools to assess and gain insight into the error propagation dynamics of fault-tolerant distributed architectures. In [3] we proposed an approach to assess system **resilience**, which we defined as the ability to contain and recover from fault effects. The **threats** to the delivery of proper system service are internal system conditions or external environmental conditions (e.g., HIRF, lightning, high-energy particle radiation, power system transients, etc.) that may cause faults in the system. There is special interest in examining the response to functional **upsets**, which are error modes that involve no permanent component damage, can simultaneously occur in multiple channels of a redundant distributed system and can cause unrecoverable state error conditions [4, 5, 6].

Under the proposed assessment approach, the system is viewed from a stimulus-response (i.e., cause and effect) perspective (see Figure 1 and Figure 2). The threat conditions specify the **stimulus space**, which is a subset of all possible system threat patterns. A **disturbance** is an external system stimulus that may cause a **perturbation**, defined here as an internal fault condition in the form of outages on the services provided by the components. Alternatively, the specification of the disturbance can be bypassed and the stimulus can be specified as a perturbation. The effects of a perturbation (i.e., errors) may propagate throughout the system and reach the external functional interface, thus causing an outage of the external system service, which we refer to as a **disruption**. The **response space** is the set of system disruptions resulting from the application of the stimulus space. As Figure 2 suggests, for a given perturbation, the severity of the disruption is determined by the error propagation characteristics of the system.

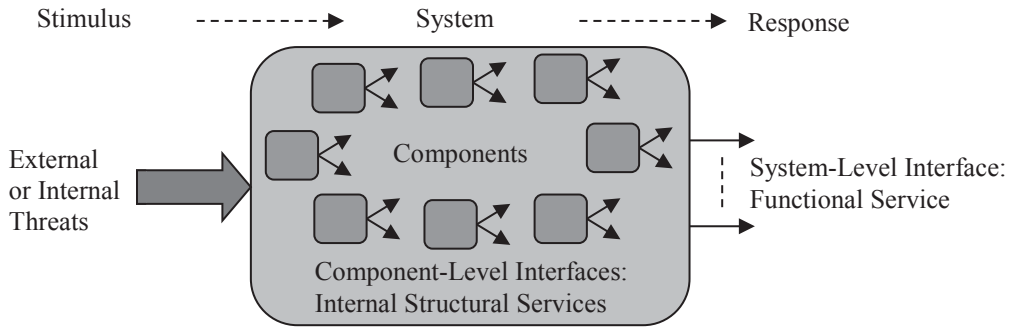

Figure 1: Stimulus-response system model

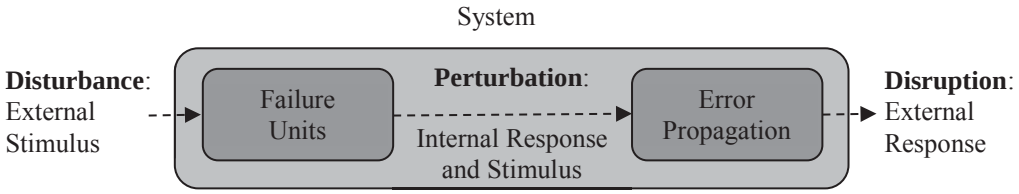

Figure 2: Stimulus-response chain

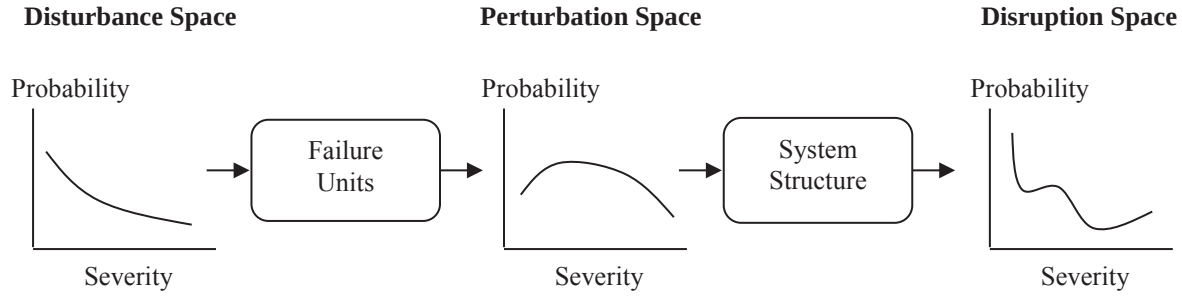

Figure 3: Description of spaces in the stimulus-response chain using probability distributions

For a quantitative system resilience analysis, the disturbance, perturbation and disruption spaces may be described in terms of probability distributions (PDs) of random variables whose values correspond to the severity of occurrences (i.e., events or instances) in these spaces. Figure 3 illustrates the use of PDs to describe the spaces in the stimulus-response chain. To enable the use of such distributions in analyses, we need severity metrics for the occurrences in each space. A simple occurrence severity model for a HIRF disturbance was described in [7]. For perturbations and disruptions, we use the concept of **corruption**, which is defined as the amount of error in a service outage. Our proposed corruption metrics for perturbations and disruptions are presented in [3]. Given the probability distribution for a stimulus, we can perform an injection experiment (e.g., a Monte Carlo experiment) to generate a response set for which we can then compute the probability distribution. The design goal for a resilient system is to mitigate the fault space by creating an inverse relation between the probability of occurrence and the severity of effects.

As part of this effort to develop robust resilient systems, two experiments were conducted at the

NASA Langley High Intensity Radiated Field Laboratory [8] to investigate the effects of radiated electromagnetic fields on digital computer systems. During the first experiment, a prototype of an onboard data communication system was exposed to a wide range of electromagnetic field conditions to measure the effects of the radio frequency (RF) radiation on the performance of the system [9]. Figure 4 shows a typical observed system response. Every time an RF radiation burst was applied to the system, the same or similar response pattern was observed. This repetitive response led to speculation that the radiation in the chamber also had a repetitive pattern[1]. Figure 5 shows a sample of the peak-normalized electromagnetic field strength measured by an antenna inside the chamber. The field amplitude pattern was indeed found to be repetitive and dependent on chamber conditions like frequency, input power and others. Based on this, it was conjectured that the error burst pattern was caused by the pattern of field excursions above the susceptibility threshold of the radiated device. We refer to these excursions of the field strength amplitude as **overstrokes**. Figure 7 shows an overstroke pattern generated by "slicing" a field amplitude curve at a level representing the susceptibility threshold of a device[2]. The overstroke amplitude of 0.0 corresponds to the field amplitude at the susceptibility threshold. We believe that the error rate and duration of functional error bursts are strongly correlated with the amplitude and duration of field strength excursions above the susceptibility threshold of the radiated device. This error generation mechanism could help explain the relation between field strength and error probability reported by Yates et al. [10].

A second experiment was conducted to collect field amplitude data suitable for a characterization of the electromagnetic environment in a reverberation chamber [7]. The characterization of the electromagnetic field was based on statistics of overstroke peak amplitude and duration for a range of susceptibility threshold profiles. Among the reported analyses, we considered the distribution of overstrokes for the susceptibility threshold profile measured in the first experiment. Figure 6 shows the scatter plot for the corresponding overstrokes. There are 4340 points in Figure 6. Figure 8 shows the histograms of the relative frequency distribution of overstroke peak amplitude and duration when the overall peak field strength is 20 V/m above the susceptibility threshold (E_{os} = 20 V/m).

By combining the results from these two experiments, we could develop a simple fault simulation model in which randomly generated disturbances in the form of field overstrokes are mapped to error bursts on system models. This relation between the disturbances and perturbations is a critical element in the approach described above for the characterization of system resilience with respect to a particular disturbance space [3].

The goal of the work presented in this report was to develop a random sample generator for an overstroke population described in terms of the peak and duration of the overstrokes. We want to generate random samples that are not taken directly from the given population sample but have approximately the same statistical properties. We also want the sample generation technique to be generic but easily tunable so it can be applied to any given overstroke population. To meet this goal, we applied a generic, non-parametric statistical model for field overstrokes and a simple simulation solution to generate random samples from this model.

---

[1] This is actually a well-known fact due to the repeated patterns of the stirrers, but we were not aware of it at the time of the experiment.

[2] Note that the data in Figures 4, 5, and 6 are for illustrative purposes only and they are not directly related. The data in these figures were not taken at the same time or with the same test conditions.

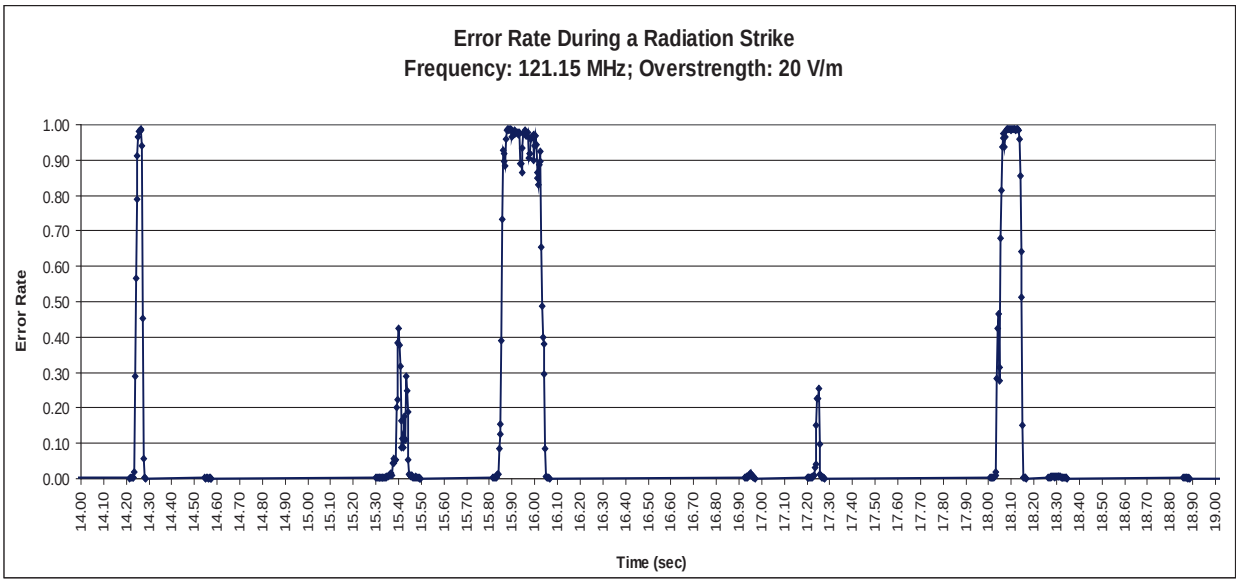

Figure 4: Example of system response to RF radiation

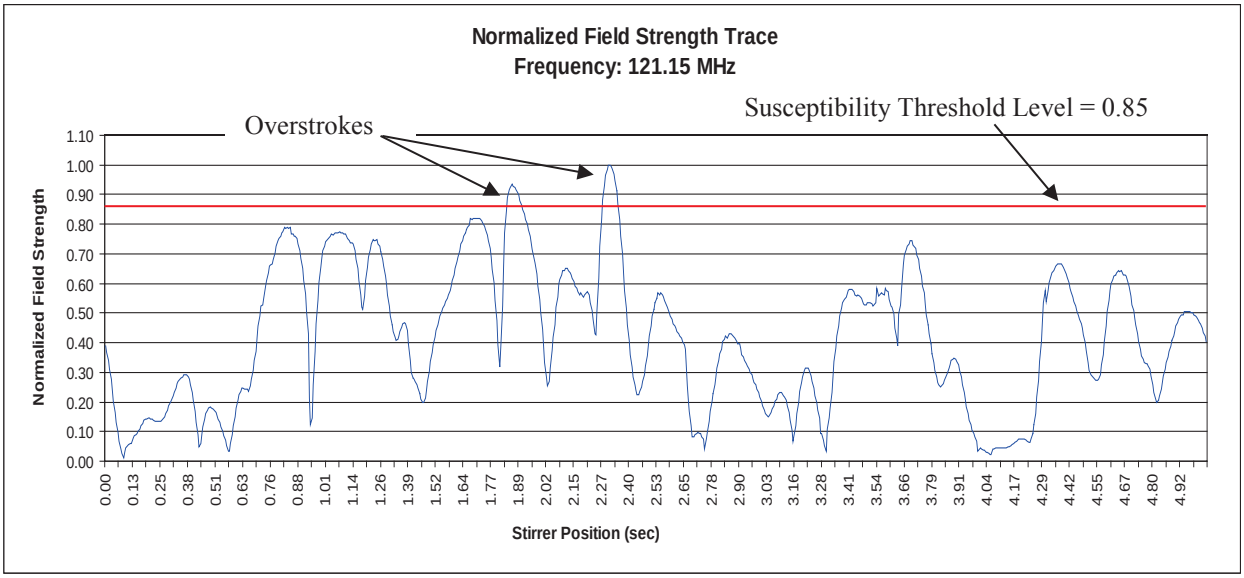

Figure 5: Sample trace of the electromagnetic field strength in a reverberation chamber

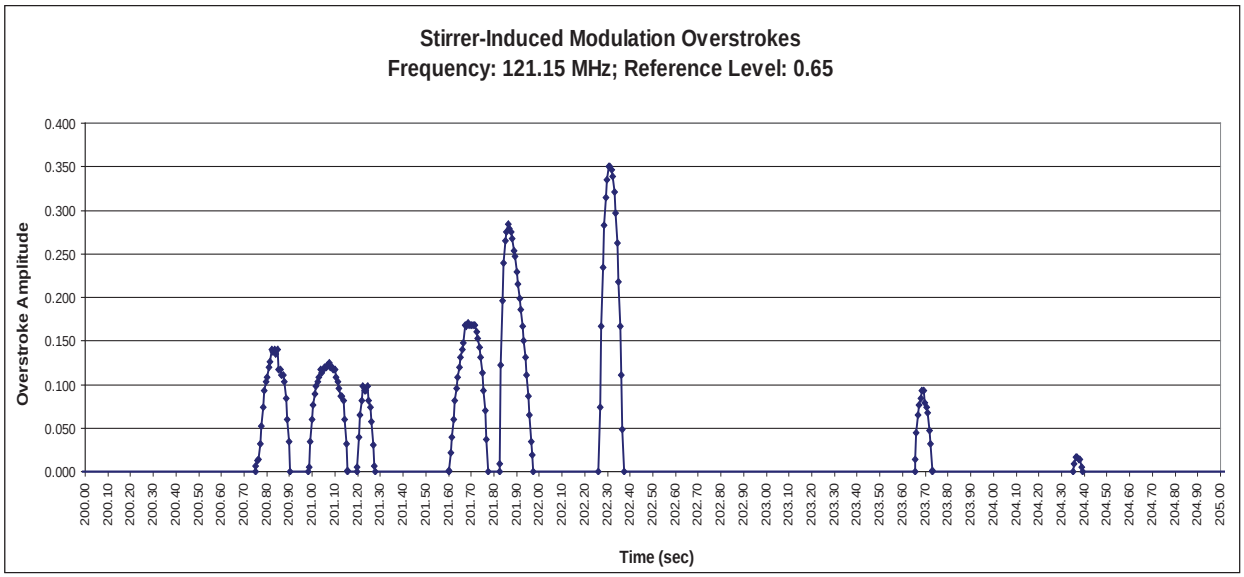

Figure 6: Scatter plot of normalized experimental overstroke peak amplitude and duration

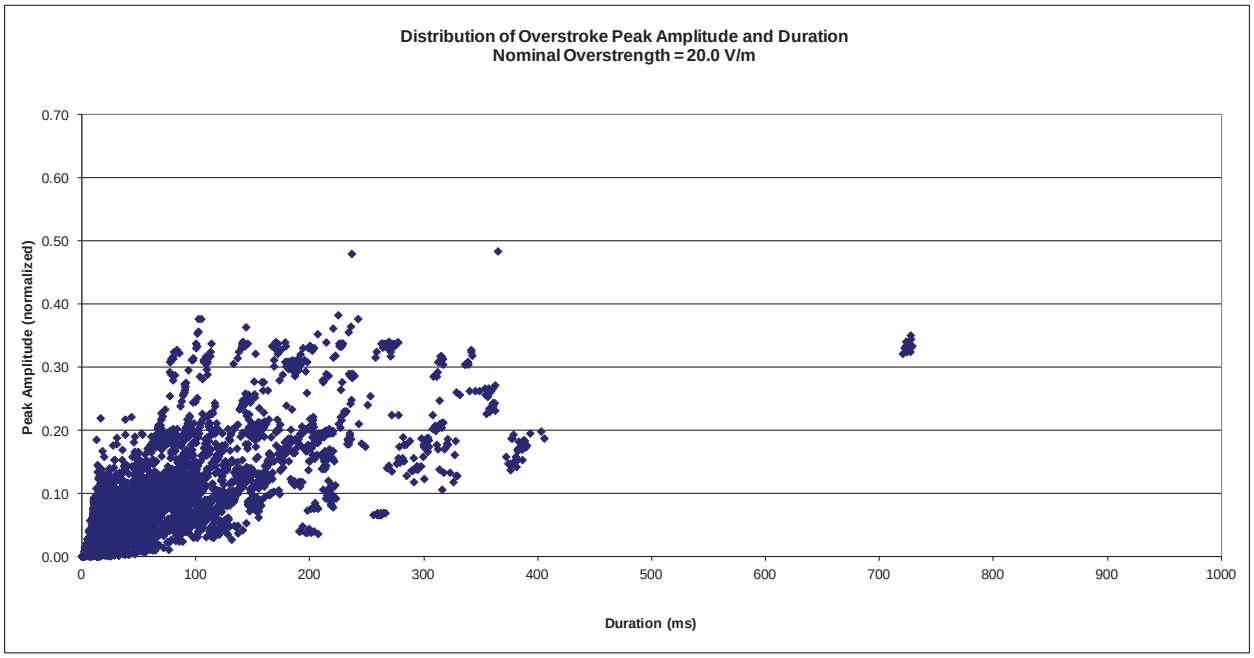

Figure 7: Example of overstrokes for a particular susceptibility threshold level

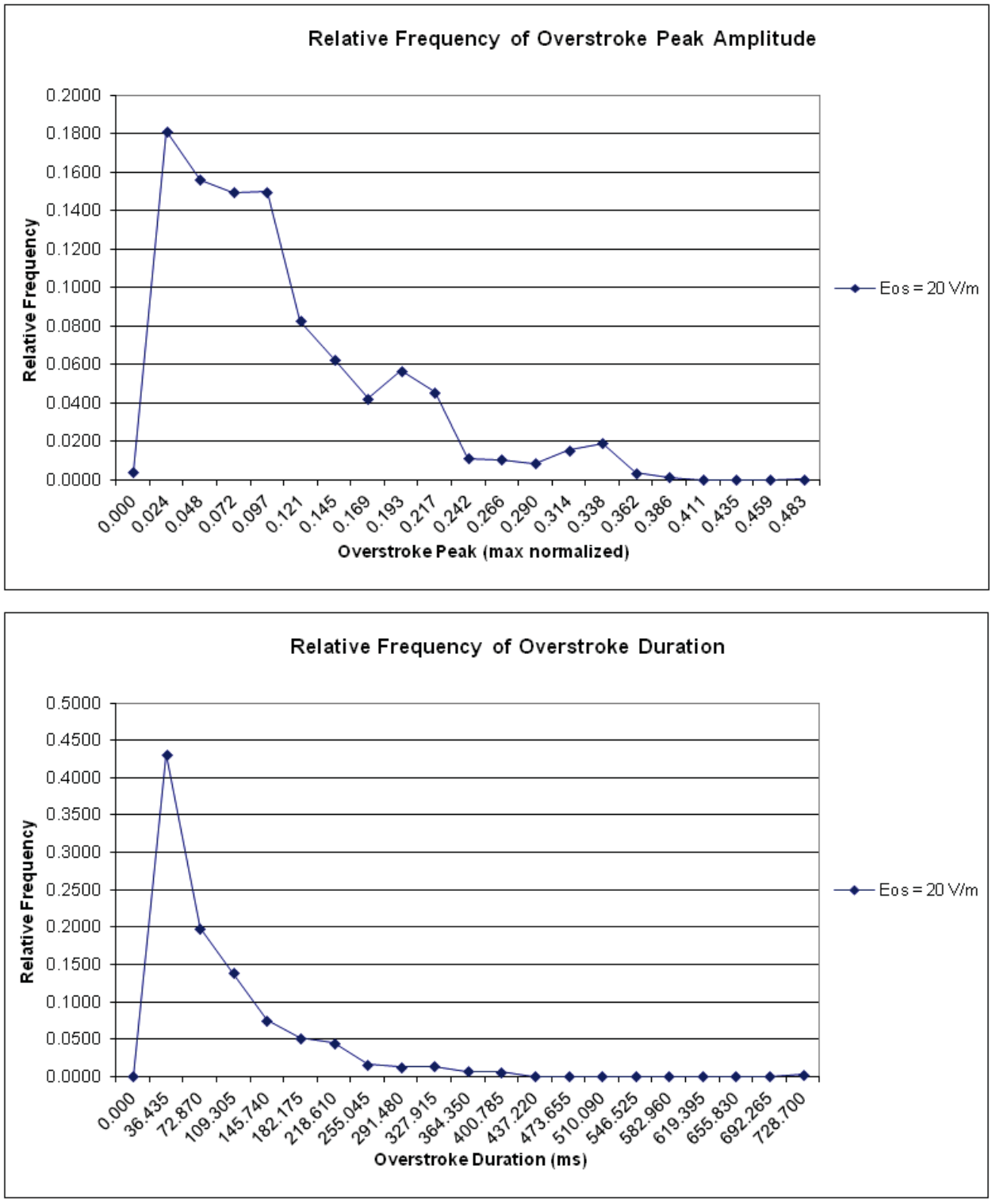

Figure 8: Histograms of experimental overstroke amplitude and duration

The next section describes the selected approach. This is followed by a description of the results. The report ends with brief concluding remarks summarizing what has been accomplished and future work.

2. Modeling Approach

A primary constraint in this study was that only the existing experimental field data as reported in [7] was available for modeling and simulation activities. It was possible to generate samples of different overstroke populations with the existing data (for example, by changing the susceptibility threshold used to determine the overstrokes from the existing field amplitude traces), but there was only one set of overstrokes for any given population as defined by the parameter configuration used to generate the overstrokes from field amplitude traces. This could be an issue if we tried to assess the absolute accuracy of the developed model. Since this was not a hypothesis testing study [11], the assessment of representativeness of a given experimental overstroke sample was not within the scope of the study. Rather, the problem was framed such that we had to determine how well the distribution of simulated overstrokes matched a given experimental sample distribution (i.e., compare experimental vs. simulated samples), assuming that the given sample was representative of the disturbance pattern that an actual system would experience in a reverberation chamber. Only the overstroke sample shown in Figure 6 was considered in this study.

An overstroke population is characterized in terms of two continuous random variables, the peak amplitude P and the duration D, and a bivariate probability distribution. An overstroke observation consists of a pair (p, d) corresponding to the peak amplitude and duration of the overstroke. For the empirical sample, P and D have ranges [0, p_{max}] and [0, d_{max}].

The first modeling approach considered was the use of empirical marginal cumulative distribution functions (CDF) for the variables P and D, and an empirical copula[3] to capture the dependence between P and D in terms of a joint cumulative distribution function for the marginal CDFs [12]. Although simple in concept, this approach was more complex to model and simulate than the alternative approaches.

The second alternative modeling approach was an empirical bivariate cumulative distribution function (eCDF), which is defined as [13]:

$$F_{P,D}(p, d) = [\Sigma_{\forall I}\, I(p_i \le p, d_i \le d)]/n,$$

for an n-point sample where the i-th point is denoted (p_i, d_i). I(x, y) is the indicator function, which is equal to 1 when x and y are true, and zero otherwise. This simple modeling approach would work well for our sample data. However, it was rejected because the simulation based on it was more complex than for our next alternative.

The selected modeling approach was an empirical probability distribution function (ePDF). For the bivariate case, this is simply a three-dimensional histogram with rectangular bins on the horizontal plane and the vertical dimension equal to the relative frequency of experimental points in each bin. As for the basic two-dimensional histogram, this approach works well if the sample size is large. Given that we had 4340 points in the experimental sample and most of them were concentrated close to the (0, 0) origin (see

[3] A copula is a multivariable probability distribution in which the marginal distributions are uniform.

Figure 6), the ePDF was the easiest and most effective alternative modeling approach. Additionally, as described in the next section, there were at least two simple techniques that could be applied to generate random samples based on the ePDF.

To build a bivariate ePDF, we had to specify the number and width of the bins. Two options were considered for the number of bins [14]. The selected option was the square-root rule, where the number of bins is given by:

$k = \sqrt{n}$.

With this choice, the growth in the size of the model (i.e., its complexity) is sub-linear relative to the number of sample points.

For the bin width selection to work in combination with the square-root rule for the number of bins, we considered two alternatives: constant bin widths and percentile-based bin widths. For the constant bin width option, the bin widths for P and D, denoted h_p and h_d, are given by:

$h_p = p_{max}/k$ and $h_d = d_{max}/k$.

The percentile-based bin width option is intended to give the model a higher resolution around the intervals with the highest concentration of points. For this bin-width alternative, the upper bound of the bin corresponding to the p-th percentile for the P random variable is given by the i-th value of P when arranged in increasing order:

$i = \text{Round}(p(n+1)/100)$.

The bin widths are determined independently for the ranges of the P and D random variables.

The results presented in Section 4 show that the empirical probability distribution function using the square-root rule and constant bin widths is an adequate model for our experimental sample distribution.

Alternatively, we can use the Freedman-Diaconis rule with constant bin width given by:

$h = 2\ (IQR/n^{1/3})$

where IQR is the inter-quartile range (i.e., the distance between the 25^{th} and 75^{th} percentiles). This bin width takes into consideration the actual distribution of the sample and is insensitive to outliers. This rule would be applied independently to the peak P and distribution D random variables to determine the dimensions of the bins. The Freedman-Diaconis rule is available for future use, if needed, but it was not implemented in the model and simulations presented in this report.

3. Simulation Approach

Simulation is simply the dynamic generation of samples from the modeled population. This is realized by a mathematical transformation based on the modeled population that takes uniform random variables as inputs and generates random variables with the desired distribution. One or more pseudo-random number generators (PRNGs) are used to produce samples of uniformly distributed variables. There are a

number of techniques that can be used to transform uniform random samples into the desired population, including Rejection Sampling, Inverse Transform Sampling, Metropolis-Hasting algorithm, Gibbs sampling, Slice sampling, and others [15]. The main difficulty for our simulation problem is that the random variables that characterize the overstroke population, P and D, are not independent, and thus, we need a way to accurately capture their correlation. In addition, we wanted our simulation approach to require only a few simple mathematical operations, be easy to implement and be computationally fast. We considered two sampling techniques: Rejection Sampling and Inverse Transform Sampling.

Rejection Sampling (also known as Acceptance-Rejection Method) can be easily understood using Figure 9. Suppose we had a random variable r with range [0, 1] and PDF given by the red line. Let u1 and u2 denote two uniform and independent (i.e., uncorrelated) random variables, both with range [0, 1]. If we generate uniformly distributed random samples in the u1 x u2 space and we discard all samples above the red line, the samples that remain are distributed according to the PDF of r. In effect, this algorithm transforms u1 and u2 into r.

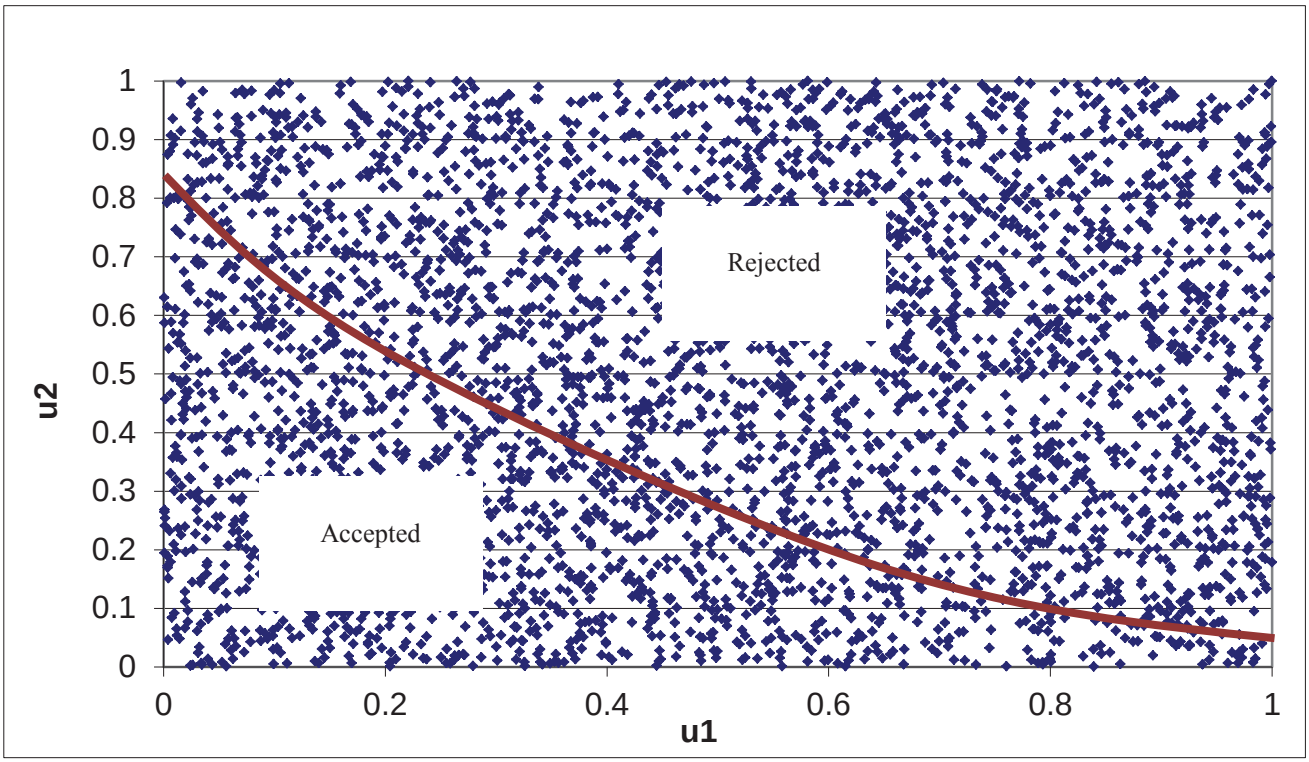

Figure 9: Illustration of Rejection Sampling concept

To apply Rejection Sampling to the overstroke bivariate distribution, we transform three uniform and uncorrelated random variables U_1, U_2, U_3 into correlated variables P and D using the empirical PDF as the rejection threshold. Specifically, sample point (p, d) is given by:

$p = p_{max} \cdot u_1$, and

$d = d_{max} \cdot u_2$.

Let $f_{P,D}(p, d)$ denote the overstroke PDF at point (p, d). If $u_3 > f_{P,D}(p, d)$, point (p, d) is rejected; otherwise, (p, d) is accepted. Comparison with $f_{P,D}(p, d)$ ensures that P and D are properly correlated.

Application of the Rejection Sampling technique requires the evaluation of $f_{P,D}(p, d)$ at every point in the P x D space as sample points (p, d) computed from variables U_1 and U_2 have continuous, real-valued ranges. We used the bilinear interpolation technique to extend our ePDF model from a discrete domain to a continuous domain. We use Figure 10 to illustrate the application of bilinear interpolation to determine the value of $Q = f_{P,D}(p, d)$. In Figure 10, we are operating in a three-dimensional space and we have four known reference points defined by our ePDF model: (p_1, d_1, Q_{11}), (p_2, d_1, Q_{21}), (p_1, d_2, Q_{12}), and (p_2, d_2, Q_{22}). We assume that $p_1 < p < p_2$ and $d_1 < d < d_2$. To determine Q, we first interpolate along the horizontal dimension in Figure 10 and then along the vertical dimension. We define four scaling factors:

$$w_{p1} = (p - p_1)/(p_2 - p_1)$$

$$w_{p2} = (p_2 - p)/(p_2 - p_1)$$

$$w_{d1} = (d - d_1)/(d_2 - d_1)$$

$$w_{d2} = (d_2 - d)/(d_2 - d_1)$$

We interpolate along the horizontal dimension to determine R_1 and R_2:

$$R_1 = w_{p2}Q_{11} + w_{p1}Q_{21}$$

$$R_2 = w_{p2}Q_{12} + w_{p1}Q_{22}$$

Next, we interpolate along the vertical dimension to determine Q:

$$Q = w_{d2}R_1 + w_{d1}R_2 = w_{p2}w_{d2}Q_{11} + w_{p1}w_{d2}Q_{21} + w_{p2}w_{d1}Q_{12} + w_{p1}w_{d1}Q_{22}$$

The corresponding equations for Q when $p = p_2$ and/or $d = d_2$ require interpolation along at most one dimension and are easily derived.

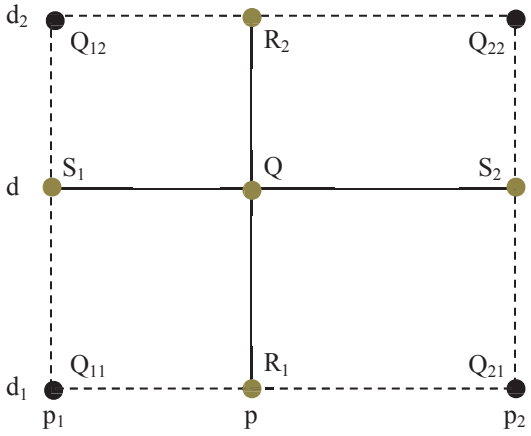

Figure 10: Reference points of bilinear interpolation technique

Our second simulation technique was a form of Inverse Transform Sampling applied to a bivariate distribution. Inverse Transform Sampling relies on the Probability Integral Transform (PIT) [16]. Let P and U denote random variables, and $F_P(P)$ denote the marginal CDF of P. If $U = F_P(P)$, then U has a uniform distribution with range [0, 1]. For the Inverse Transform Sampling technique, we apply the PIT transform in the opposite direction: $P = F_P^{-1}(U)$. This is illustrated in Figure 11 where we use the random value u to graphically determine the corresponding value p. To expand the inverse transform to the bivariate case, we use two uniform random variables U1 and U2. First, we apply the inverse transform to the marginal CDF of P:

$$p = F_P^{-1}(u_1)$$

Then, we apply the inverse transform to the conditional CDF of d, denoted $F_{D|P}(d|p)$:

$$d = F_{D|P}^{-1}(u_2|p)$$

The marginal $F_P(P)$ is simply a cumulative histogram of the overstroke sample set considering only the P values. The number of bins was set using the same square-root rule as for the ePDF model. For the conditional CDF of d, $F_{D|P}(d|p)$, we applied bilinear interpolations to the ePDF to determine the conditional PDF of d given p, denoted $f_{D|P}(d|p)$, and then computed the conditional CDF, $F_{D|P}(d|p)$.

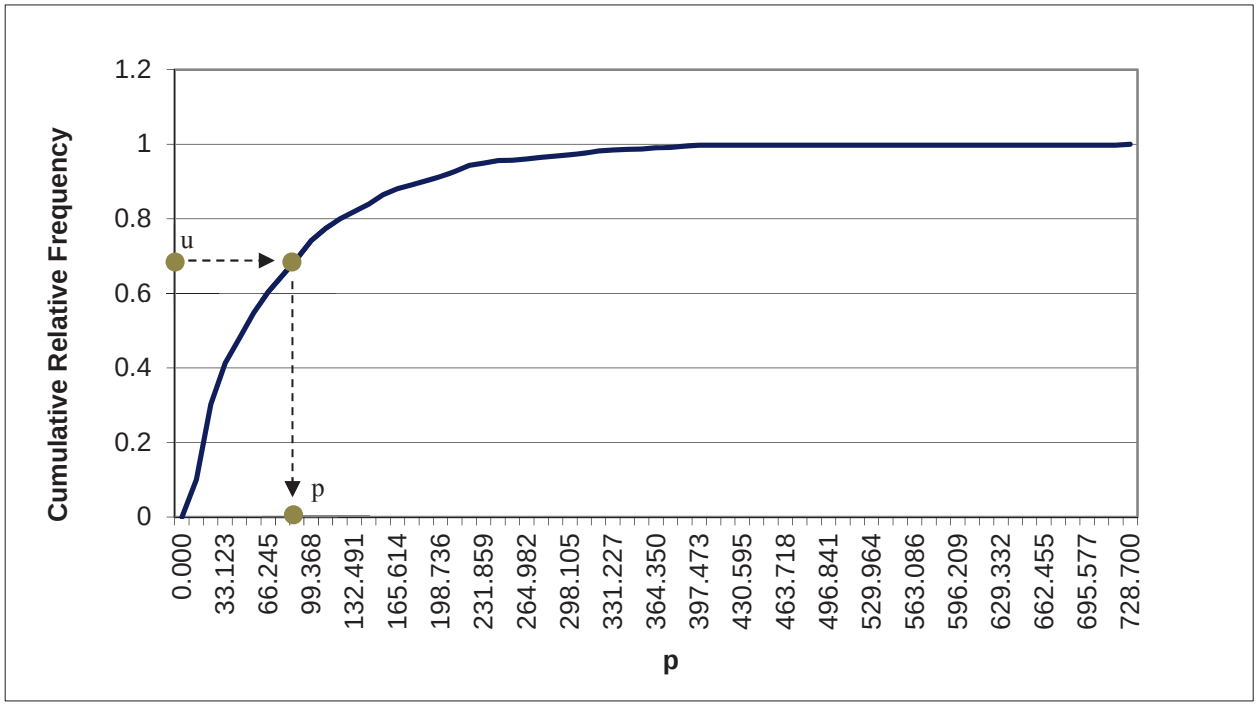

Figure 11: Illustration of Inverse Transform Sampling

4. Results

The results cover the aspects of modeling and simulation, including pseudo-random number generation, and comparison of Rejection Sampling and Inverse Transform Sampling. We created C language programs to produce the ePDF model and simulate it to generate random samples.

4.1. Empirical Probability Distribution Function

Figure 12 shows the ePDF using the square-root rule and constant bin widths. The results presented below show that this is an adequate model for our experimental sample distribution.

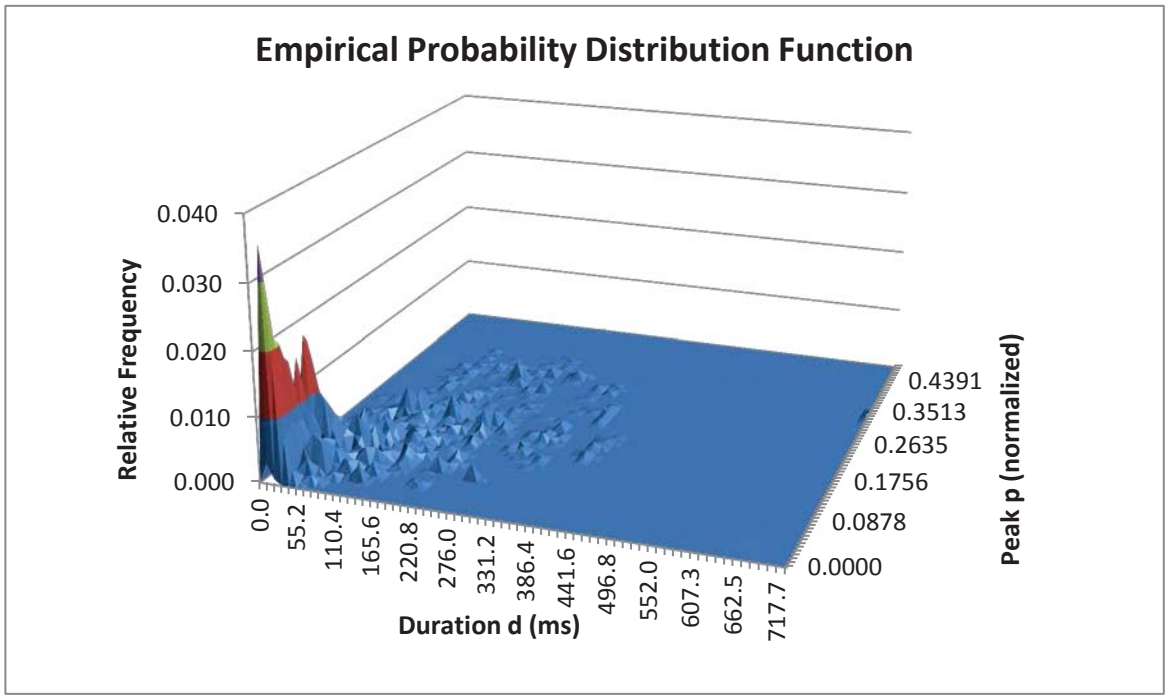

Figure 12: Empirical Probability Density Function

4.2. Pseudo-Random Number Generator

The simulation of the model requires pseudo-random number generators (PRNGs) whose output are approximately uniform and uncorrelated between samples and between generators. Figure 13 shows the PDF for a PRNG. As expected, each of the 10 bins contains approximately one-tenth of the generated random numbers. Figure 14 shows that the cumulative distribution function of the PRNGs grows linearly, as expected for a uniform random variable. Figure 15 shows a scatter plot where the point coordinates are the outputs of two PRNGs: (PRNG1, PRNG2). This figure shows that there is no discernible pattern of correlation between the PRNGs. These results provide confidence that the PRNGs, as the foundation for our simulation approach, meet the basic requirements of uniformity and independence.

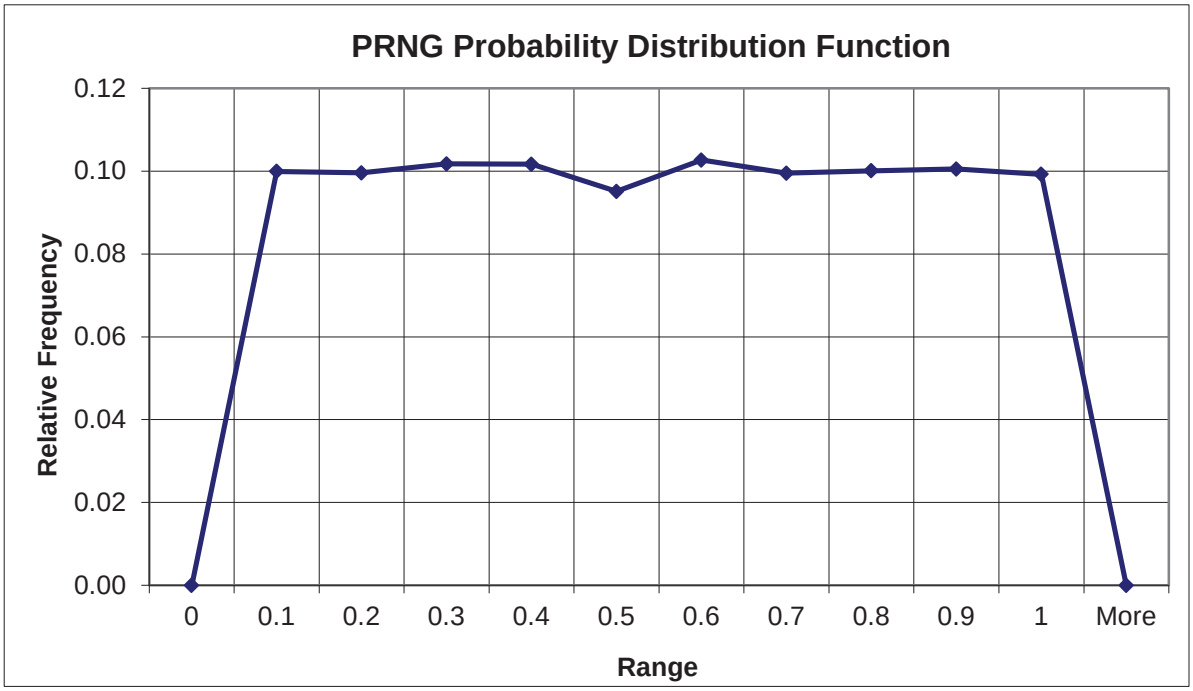

Figure 13: Cumulative distribution function for sample of pseudo-random number generator

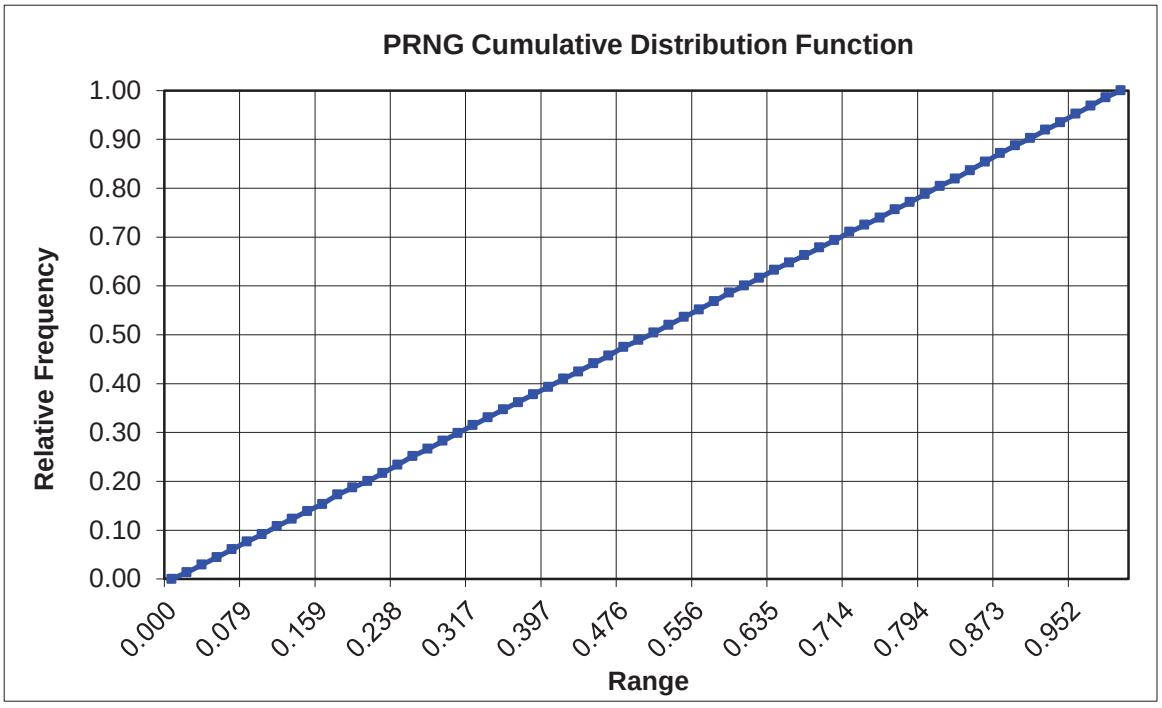

Figure 14: Probability distribution function for sample output of pseudo-random number generator

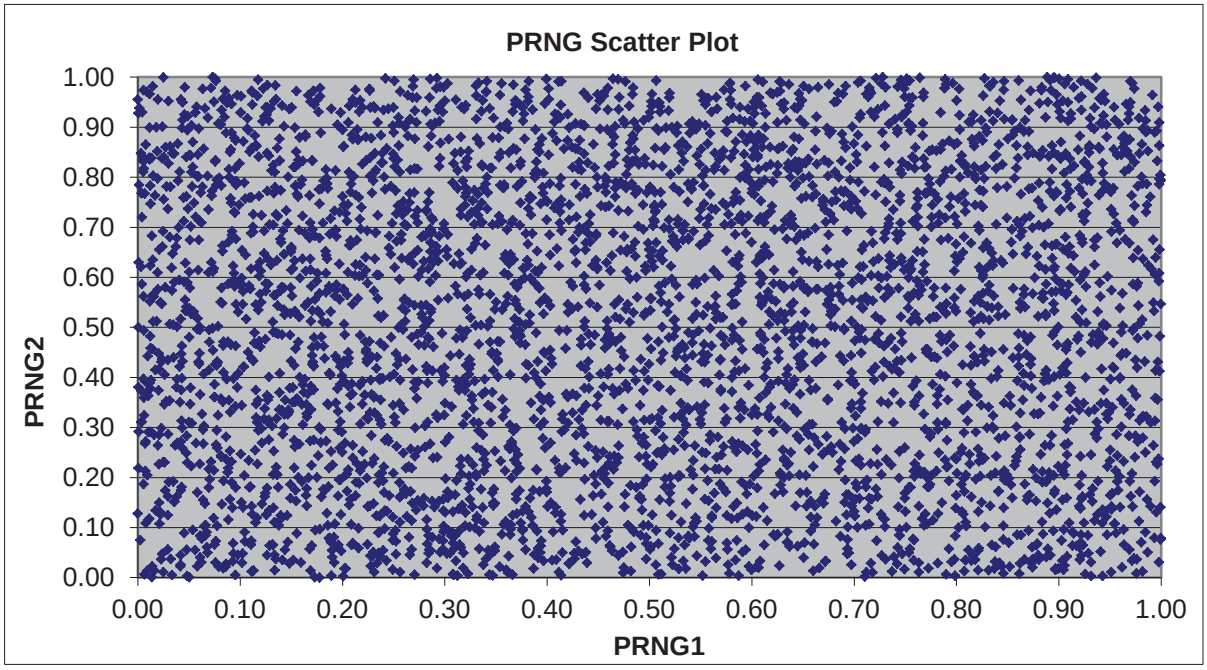

Figure 15: Scatter plot for two PRNGs

4.3. Overstroke Sample Generation

The experimental samples and the samples generated by the R ejection Sampling and Inverse Transform Sampling techniques are shown in Figures 16 to 18. The corresponding marginal CDFs for the overstroke peak p and duration d are given in Figures 19 and 20, respectively. Visual inspection of these figures appears to indicate that the Inverse Transform Sampling technique has slightly better fidelity. The following section gives objective measures of goodness-of-fit for both simulation techniques.

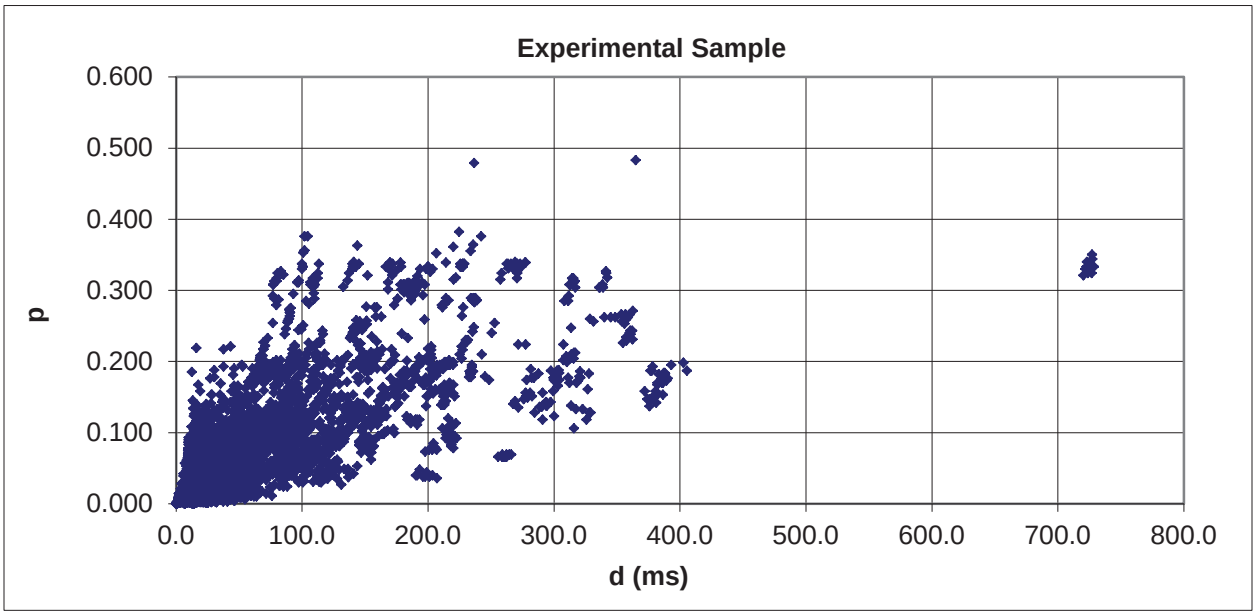

Figure 16: Experimental overstroke samples

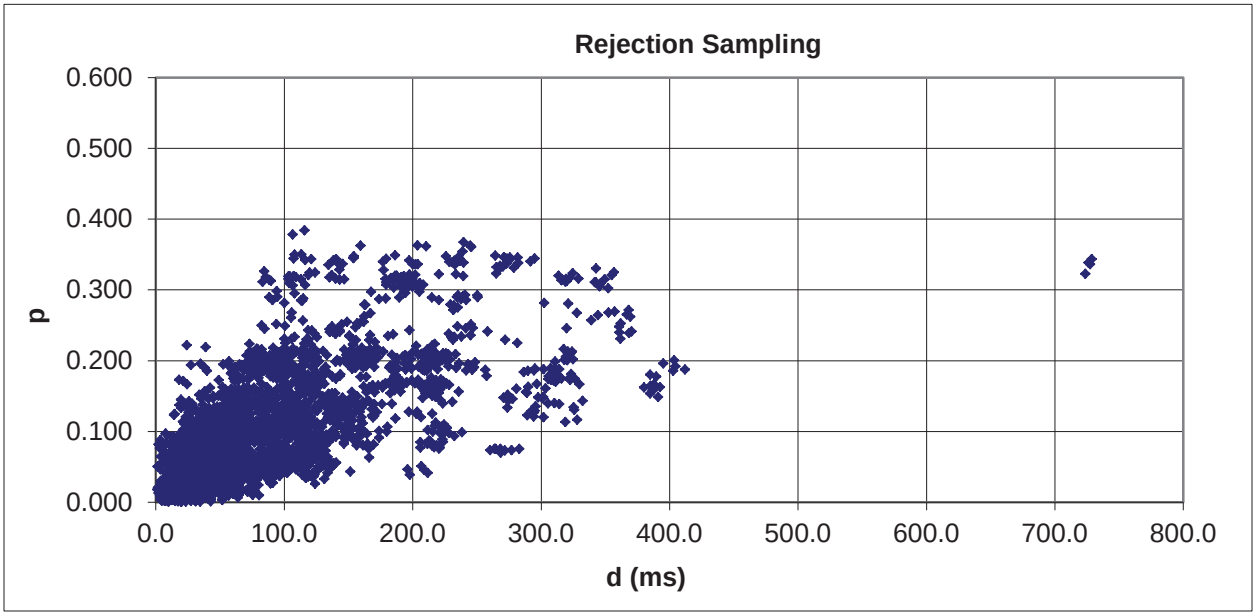

Figure 17: Samples generated by Rejection Sampling technique

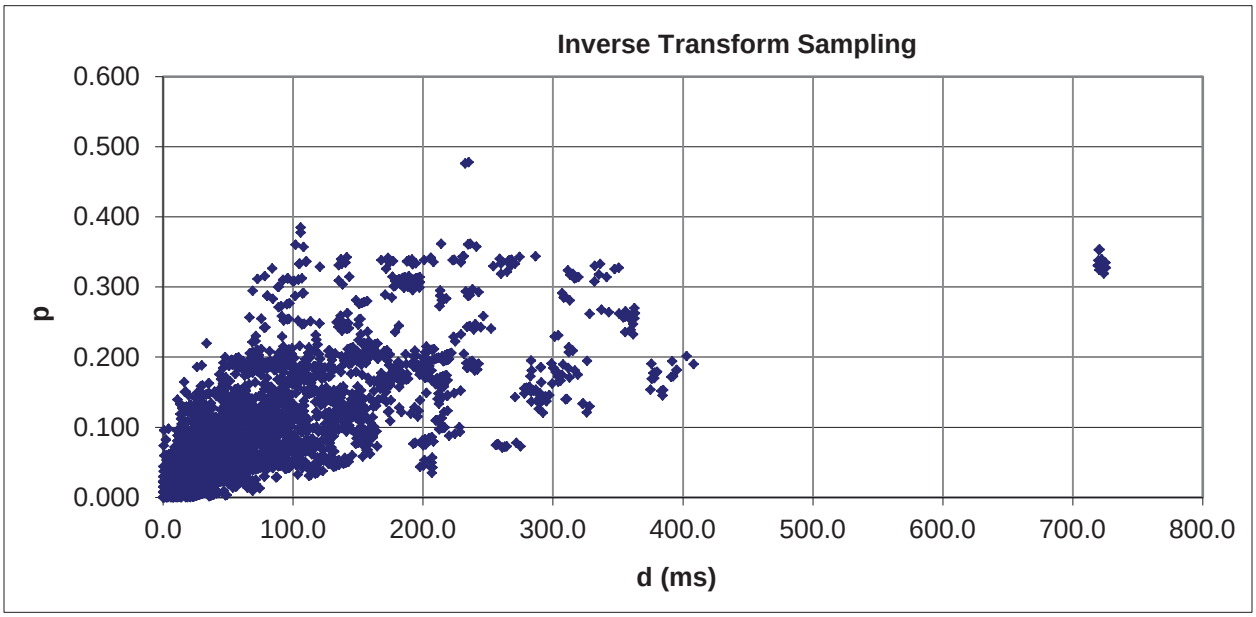

Figure 18: Samples generated by Inverse Transform Sampling technique

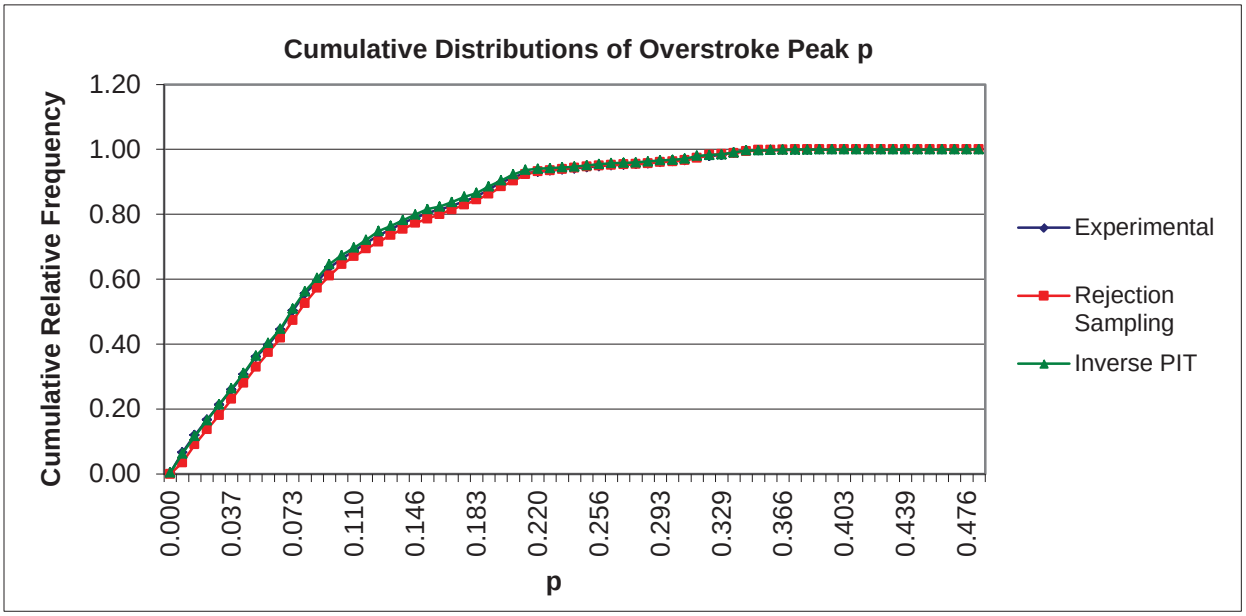

Figure 19: Marginal CDF of overstroke peak p for experimental and simulation samples

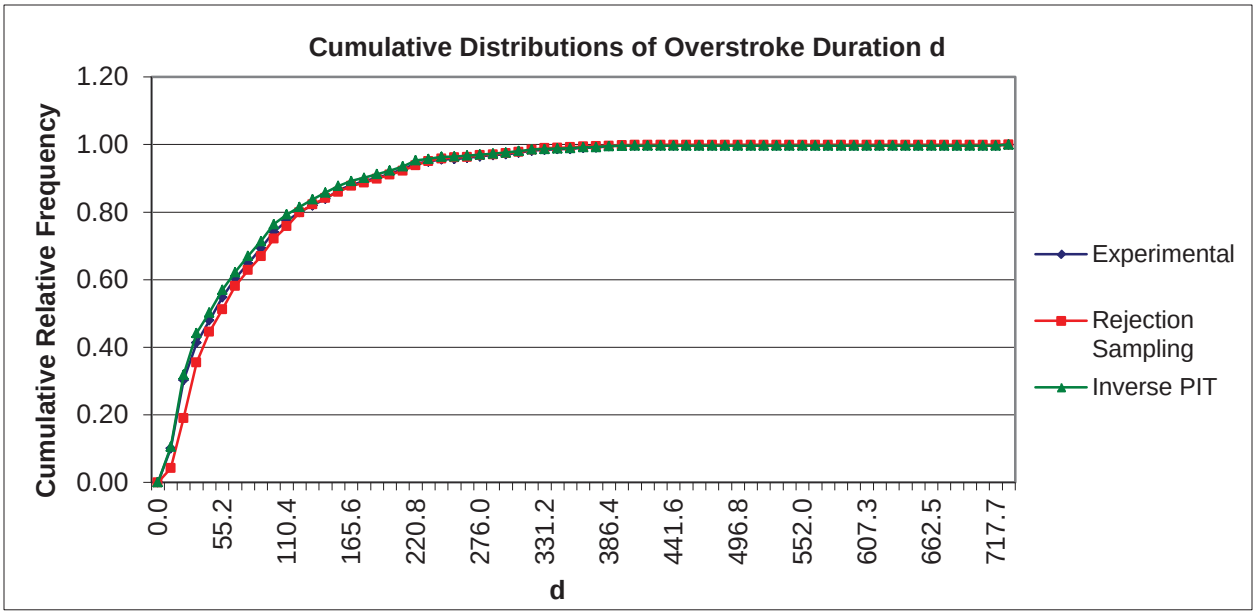

Figure 20: Marginal CDF of overstroke duration d for experimental and simulation samples

4.4. Goodness-of-Fit Measures

The goodness of fit (GoF) of the simulation samples was evaluated quantitatively using the Chi-Square test [16, 17] applied to the marginal CDFs for p and d of the generated samples using 10 cells, corresponding to 9 degrees of freedom. The expected observed frequency was based on the experimental sample. The cell (or bin) widths were defined such that each bin covered 10% of the points in the original experimental sample. As the Chi-Square statistics in Table 1 show, the Inverse Transform Sampling technique performed much better for both p and d than the Rejection Sampling technique. It is not clear why Inverse Transform Sampling had better results, though we suspect this may be due to some sort of smoothing effect in the Inverse Probability Integral Transform (IPIT) that minimizes the slight residual clustering patterns (i.e., correlation) in the PRNG outputs visible in Figure 15. The Rejection Sampling technique simply accepts or rejects generated (p, d) points with no significant mathematical transformation between the PRNG outputs and the points.

Table 1: Chi-Square Test results for marginal CDFs (9 degrees of freedom)

Overstroke Parameter	Simulation Technique	Chi-Square Statistic	Significance
Peak p	Rejection Sampling	47.81	2.78e-07
	Inverse Transform Sampling	**7.36**	0.60
Duration d	Rejection Sampling	376.22	1.51e-75
	Inverse Transform Sampling	**15.56**	0.08

5. Conclusions

We have described a general modeling and simulation approach for a typical disturbance pattern that a digital device may experience in an electromagnetic reverberation chamber. The modeling approach is based on a three-dimensional histogram using bilinear interpolation to build a continuous surface for the empirical probability distribution function. We considered two simulation approaches extended to the case of a bivariate distribution: Rejection Sampling and Inverse Transform Sampling. The results showed that the Inverse Transform Sampling technique can generate samples that most closely match the empirical distribution.

We intend to apply this modeling and simulation approach to generate random disturbance patterns as stimulus in a system fault-response simulator. The purpose of the simulator is to gain a thorough understanding of the relation between internal upsets and the propagated effects observable at the external system interface. To achieve this, we needed to develop a technique to map disturbances to internal perturbations of the system failure units (see Figure 3). We also need to develop error propagation models that determine the system-structure-dependent transformation from internal perturbations to external disruptions (see Figure 2). The ultimate goal is to develop a model-based methodology to assess system fault response and guide design efforts for enhanced resilience in complex safety-critical distributed systems.

References

[1] Federal Aviation Administration. http://www.faa.gov/nextgen/ Accessed February 24, 2014.

[2] Driscoll, Kevin, et al.: *Data Network Criteria Evaluation Report*. Federal Aviation Administration, DOT/FAA/AR-09/27, July 2009.

[3] Torres-Pomales, Wilfredo: *An Approach for the Assessment of System Upset Resilience*. NASA/TM-2013-217798, January 2013.

[4] Belcastro, Celeste M.: *Laboratory Test Methodology for Evaluating the Effects of Electromagnetic Disturbances on Fault-Tolerant Control Systems*. NASA Technical Memorandum 101665, November 1989.

[5] Fuller, Gerald L.: *Understanding HIRF – High Intensity Radiated Fields*. Aviation Communications, Inc., Leesburg, VA, 1995, p. 7-2.

[6] Hess, Richard: *Computing Platform Architectures for Robust Operation in the Presence of Lightning and Other Electromagnetic Threats.* 16th Digital Avionics Systems Conference (DASC), 1997.

[7] Torres-Pomales, W.: *Analysis of the Radiated Field in an Electromagnetic Reverberation Chamber as an Upset-Inducing Stimulus for Digital Systems*. NASA/TM-2012-217789, December 2012.

[8] Williams, R. A.: *The NASA High Intensity Radiated Fields Laboratory*. 16th Digital Avionics Systems Conference, October 1997.

[9] Torres-Pomales, Wilfredo: *Characterization of the HIRF Susceptibility Threshold for a Prototype Implementation of an Onboard Data Network*. NASA/TM-2012-217754, August 2012.

[10] Yates, A.M.; et al.: *High-Intensity Radiated Field Fault-Injection Experiment for a Fault-Tolerant Distributed Communication System*. IEEE/AIAA 29th Digital Avionics Systems Conference (DASC), October 2010, pp. 4.E.301 – 4.E.3-15.

[11] Mendenhall, W. and Sincich, T.: *Statistics for Engineering and the Sciences*. 5th Edition, Prentice Hall, 2006.

[12] Nelsen, Roger B.: *An Introduction to Copulas*. 2nd Edition, Springer, 2007.

[13] van der Vaart, A. W.: *Asymptotic Statistics*. Cambridge University Press, 2000.

[14] Scott, David W.: *Multivariate Density Estimation: Theory, Practice, and Visualization*. 1st Edition, Wiley, 1992.

[15] Fishman, George: *Monte Carlo: Concepts, Algorithms, and Applications*. Springer, 2011.

[16] Barnes, J. Wesley: *Statistical Analysis For Engineers*. Prentice Hall, 1988.

[17] Greenwood, Priscilla E.; and Nikulin, Michael S. *A Guide to Chi-Squared Testing*. Wiley-Interscience, 1996.

Abbreviations

CDF	Cumulative Distribution Function
eCDF	Empirical Cumulative Distribution Function
ePDF	Empirical Probability Distribution Function
GoF	Goodness of Fit
HIRF	High Intensity Radiated Field
IPIT	Inverse Probability Integral Transform
ms	Millisecond
NASA	National Aeronautics and Space Administration
PD	Probability Distribution
PDF	Probability Distribution Function
PIT	Probability Integral Transform
PRNG	Pseudo-Random Number Generator
V&V	Validation and Verification

REPORT DOCUMENTATION PAGE

Form Approved
OMB No. 0704-0188

The public reporting burden for this collection of information is estimated to average 1 hour per response, including the time for reviewing instructions, searching existing data sources, gathering and maintaining the data needed, and completing and reviewing the collection of information. Send comments regarding this burden estimate or any other aspect of this collection of information, including suggestions for reducing this burden, to Department of Defense, Washington Headquarters Services, Directorate for Information Operations and Reports (0704-0188), 1215 Jefferson Davis Highway, Suite 1204, Arlington, VA 22202-4302. Respondents should be aware that notwithstanding any other provision of law, no person shall be subject to any penalty for failing to comply with a collection of information if it does not display a currently valid OMB control number.
PLEASE DO NOT RETURN YOUR FORM TO THE ABOVE ADDRESS.

1. REPORT DATE *(DD-MM-YYYY)*	2. REPORT TYPE	3. DATES COVERED *(From - To)*
01- 04 - 2014	Technical Memorandum	

4. TITLE AND SUBTITLE

Modeling and Simulation of Upset-Inducing Disturbances for Digital Systems in an Electromagnetic Reverberation Chamber

5a. CONTRACT NUMBER

5b. GRANT NUMBER

5c. PROGRAM ELEMENT NUMBER

6. AUTHOR(S)

Torres-Pomales, Wilfredo

5d. PROJECT NUMBER

5e. TASK NUMBER

5f. WORK UNIT NUMBER

534723.02.02.07.30

7. PERFORMING ORGANIZATION NAME(S) AND ADDRESS(ES)

NASA Langley Research Center
Hampton, VA 23681-2199

8. PERFORMING ORGANIZATION REPORT NUMBER

L-20380

9. SPONSORING/MONITORING AGENCY NAME(S) AND ADDRESS(ES)

National Aeronautics and Space Administration
Washington, DC 20546-0001

10. SPONSOR/MONITOR'S ACRONYM(S)

NASA

11. SPONSOR/MONITOR'S REPORT NUMBER(S)

NASA/TM-2014-218243

12. DISTRIBUTION/AVAILABILITY STATEMENT

Unclassified - Unlimited
Subject Category 33
Availability: NASA CASI (443) 757-5802

13. SUPPLEMENTARY NOTES

14. ABSTRACT

This report describes a modeling and simulation approach for disturbance patterns representative of the environment experienced by a digital system in an electromagnetic reverberation chamber. The disturbance is modeled by a multi-variate statistical distribution based on empirical observations. Extended versions of the Rejection Samping and Inverse Transform Sampling techniques are developed to generate multi-variate random samples of the disturbance. The results show that Inverse Transform Sampling returns samples with higher fidelity relative to the empirical distribution. This work is part of an ongoing effort to develop a resilience assessment methodology for complex safety-critical distributed systems.

15. SUBJECT TERMS

Modeling; Safety; Simulation

16. SECURITY CLASSIFICATION OF:			17. LIMITATION OF ABSTRACT	18. NUMBER OF PAGES	19a. NAME OF RESPONSIBLE PERSON
a. REPORT	b. ABSTRACT	c. THIS PAGE			STI Help Desk (email: help@sti.nasa.gov)
					19b. TELEPHONE NUMBER *(Include area code)*
U	U	U	UU	27	(443) 757-5802